Topography and energy variation in physisorbed layers

L. W. Bruch
Department of Physics, University of Wisconsin–Madison, Madison, Wisconsin 53706, USA
(Received 14 May 2003; revised manuscript received 10 September 2003; published 31 December 2003)

The combined effects on the monolayer dynamics of the lateral energy variation (corrugation) of the adatom-substrate potential and of the variation of adatom heights above the substrate, within the monolayer solid, are treated for three examples: Ar/graphite, Kr/graphite, and H_2/MgO(001). For inert gases, the effects are shown to offset each other and result in nearly dispersionless *S*-mode branches, for adatom vibrations perpendicular to the substrate, similar to those observed for most physically adsorbed monolayers. For the H_2/MgO(001) monolayer solids, a dispersive branch observed by inelastic helium atom scattering is assigned to an in-plane vibration and an estimate of the surface corrugation amplitude is given. Three dispersionless phonon branches observed for H_2/MgO(001) are discussed, but there is no conclusive identification of the molecular motions giving rise to those branches.

DOI: 10.1103/PhysRevB.68.235420 PACS number(s): 68.43.Pq, 63.22.+m, 67.70.+n

I. INTRODUCTION

Many properties of physically adsorbed monolayer solids are modeled successfully without much knowledge of the lateral variation of the adatom-substrate potential—i.e., the corrugation terms in the ''holding potential'' V_h—and without including the fact that the adatoms are at various heights z above the substrate.[1] The lateral variation is crucial in setting energy barriers to motion on the substrate surface and in determining Brillouin-zone-center frequency gaps in the dispersion relation for monolayer phonons.[2] The z variation, or surface topography, becomes evident in imaging experiments[3,4] and is reflected in the intensities of atoms diffracted from the layer.[5] Another signature might be a dispersion in the *S*-mode frequencies $\omega_\perp$, of adatom vibrations perpendicular to the substrate surface, arising from the fact that the atoms of an incommensurate monolayer solid are in many different substrate environments.[6] However, there is little dispersion in $\omega_\perp$ for most monolayer solids.[7,8] Thus there must be an interplay between the contributions to the curvature in V_h and the topography in z. The purpose of this paper is to demonstrate the interplay in calculations of $\omega_\perp$ for two classical examples, Ar/graphite[9] and Kr/graphite,[10] and to include it in a discussion of the assignment of modes observed[11] for the quantum monolayer solid H_2/MgO(001).

The discussion is in terms of the coefficients in the Fourier decomposition of V_h using reciprocal lattice vectors $\vec{g}$ of the substrate surface:[12]

$$V_h(\vec{r},z) = V_0(z) + \sum_{\vec{g}} V_{\vec{g}}(z)\exp(\imath\vec{g}\cdot\vec{r}), \qquad (1)$$

where the adatom position is expressed in lateral $\vec{r}$ and perpendicular z coordinates relative to a substrate atom in the surface layer. $V_0(z)$ is termed the laterally averaged holding potential and the V_g are the corrugation amplitudes. The topography arises from the fact that the z which minimizes V_h is a function of the lateral position $\vec{r}$. For physically adsorbed layers, the energy scale of V_0 is usually at least one order of magnitude larger than that of the V_g, and there is an extensive database with the overall parameters of V_0 for many adatom-substrate combinations.[14]

The effect of the leading amplitude V_{g0} at the potential minimum can be isolated in the zone-center frequency gap $\omega_{0\parallel}$ of adlayer vibrations. This has been fruitful for near-classical adsorbates, as summarized in Table I where the measured gaps and derived amplitudes are listed for several examples. For Xe/Cu(110), essentially a uniaxially incommensurate lattice, the gap[17] gives a measure of the energy variation transverse to the troughs. The quantum solid cases H_2 and ^{4}He are more difficult, because they have large effects of zero-point motion.[2] The calculations for the triangular monolayer lattices used information on the adsorption site.[21]

The body of empirical knowledge about the lateral energy variation is really quite limited. Thus, the recent inelastic atom scattering experiment[11] for H_2/MgO(001) showing a dispersive phonon branch with a zone-center gap of 2.5 meV is an important step. It will be argued in Sec. III that the gap can be assigned to vibrations along the short axis of a higher-order-commensurate unit cell and hence to a corrugation amplitude $|V_{g0}| \approx 0.47$ meV for $g = 2.12$ Å^{-1}. This is on the scale of the value inferred for H_2/graphite and of a prediction by Karimi and Vidali.[22]

The experiments[11] for monolayer H_2/MgO(001) also give a measure of the (z) topography of the layer, by analysis of diffraction intensities, and show two dispersionless branches in the phonon spectrum at about 10 meV. While a perpendicular mode at about that energy was predicted by Karimi and Vidali, the presence of two modes with splitting by about 2 meV has not been explained. It is discussed here in the context of the dispersionless *S* modes observed for Ar/graphite and Kr/graphite.

The organization of this paper is as follows: Section II contains a classical mechanical treatment of the effect of height variations on the lattice dynamics of monolayers on graphite. Section III contains a treatment of the quantum solid of H_2/MgO(001), discussing the assignment of observed phonon branches and the effects of height variations on the $\omega_\perp$ branch. Section IV contains final remarks.

TABLE I. Corrugation energy amplitude V_{g0} from Brillouin-zone-center gap frequency $\omega_{0\|}$ of monolayer lattices. The system, commensurate lattice, $\omega_{0\|}$ (in meV), wave number g_0 (in Å^{-1}) of the term that acts coherently to determine $\omega_{0\|}$, and the V_{g0} (in meV) are listed. The adlayer adsorption site, needed for deriving V_{g0} from $\omega_{0\|}$, is also given. For these triangular lattices, the frequency is related to the effective corrugation amplitude, averaged over lateral zero-point vibrations, by $\omega_{0\|}=\sqrt{(-3g^2\overline{V}_g/m)}$, where m is the adatom or admolecule mass.

System	Structure	$\omega_{0\|}$	g_0	V_{g0}	Site
Xe/Pt(111)	$\sqrt{3}$ R30°	1.3[a]	2.62	−2.6	Atop[i]
Xe/Cu(111)	$\sqrt{3}$ R30°	0.4±0.15[b]	2.84	−0.2	Atop[i]
Xe/Cu(110)	(26×2)	0.7[c]	1.74	−2.6	Row-on-row[i]
N_2/graphite	$3\times\sqrt{3}$	1.6[d]	2.95	−0.7[g]	Hexagon center[j]
H_2/graphite	$\sqrt{3}$ R30°	4.08[e]	2.95	−0.6	Hexagon center[j]
He/graphite	$\sqrt{3}$ R30°	1.0[e]	2.95	−0.13[h]	Hexagon center[j]
H_2/MgO(001)	$c(4\times2)$	2.5[f]	2.12	−0.47	[k]

[a]Reference 15.
[b]Reference 16.
[c]Reference 17.
[d]Reference 18.
[e]Reference 19.
[f]Reference 11.
[g]Calculated for spherical molecules and the $\sqrt{3}$R30° center-of-mass lattice.
[h]Reference 20.
[i]Reference 21. The adsorption geometry of Xe/Cu(110) is determined for the (12×2) lattice. V_{g0} is estimated for a classical lattice using Eq. (9) with $\eta=0$.
[j]Result for holding potentials calculated by atom-atom sums, Ref. 12; the hexagon center is at $\vec{r}=0$.
[k]Perhaps row-on-Mg rows.

II. INCOMMENSURATE MONOLAYERS ON GRAPHITE

Inelastic neutron scattering experiments[9] for a triangular incommensurate monolayer solid of Ar/graphite at 5 K with nearest-neighbor spacing $L=3.86$ Å give an S-mode frequency of 5.6 ± 0.35 meV. At this L, the argon lattice is rotated[23] by 3.1°–3.4° from the 30° axis of the graphite. For Kr/graphite with $L\simeq4.04$ Å, the S-mode frequency determined by inelastic helium atom scattering is[10] 4.1 ± 0.2 meV apart from the small-wave-number region where it hybridizes[24] with the graphite modes. The rotation angle relative to the 30° axis is[25] 1.0°–1.2°.

Both these cases appear to be incommensurate lattices. For the purpose of examining the phonon spectra they may be approximated by higher-order-commensurate (HOC) lattices.[26] This becomes a good approximation for large HOC cells, where the modulation by the corrugation is small. Let the graphite surface lattice have primitive vectors

$$\mathbf{a}_1=\ell\hat{x};\mathbf{a}_2=\ell\left(\frac{1}{2}\hat{x}+\frac{\sqrt{3}}{2}\hat{y}\right), \tag{2}$$

with $\ell=2.46$ Å, and consider the family of HOC lattices generated by the primitive vectors

$$\mathbf{A}_1=(M+1)\mathbf{a}_1+M\mathbf{a}_2,\quad \mathbf{A}_2=-M\mathbf{a}_1+(2M+1)\mathbf{a}_2. \tag{3}$$

The Bravais cell contains N^2 adatoms at positions generated initially by the vectors $\mathbf{b}_1=\mathbf{A}_1/N$, $\mathbf{b}_2=\mathbf{A}_2/N$. The average adlayer lattice is a triangular lattice with nearest-neighbor spacing $L=(1/N)\sqrt{(3M^2+3M+1)}\ell$. The incommensurate Ar/graphite can be mimicked by the HOC lattice with $M=4$ and $N=5$, having $L=3.84$ Å and rotation 3.7° relative to the 30° axis. The Kr/graphite case can be mimicked by the HOC lattice with $M=9$ and $N=10$, having $L=4.05$ Å and rotation angle 1.7°.

The adatom-adatom potentials are the HFD-B2 models used[1] for the gases on Pt(111). The holding potentials V_h are constructed[12,13] from pairwise sums of Lennard-Jones (12,6) potentials $[(\epsilon,\sigma)=(57.9\text{ K},\ 3.40\text{ Å})$ for Ar/graphite and $=(75\text{ K},\ 3.42\text{ Å})$ for Kr/graphite] with the Cole anisotropy parameters $\gamma_A=0.4$, $\gamma_R=-0.54$. The substrate is taken to be static, and the spectra are calculated with quasiharmonic lattice dynamics.[12] The z-projected density of states, also termed the ''spectral strength,'' is constructed from the $3N^2$ eigenvalues $\omega_j(\mathbf{q})$ and eigenvectors $\mathbf{e}^j$ of the dynamical matrix according to

$$\rho_z(\Omega)=\sum_q\sum_j|\mathbf{e}_z^j(\mathbf{q})|^2\delta(\omega_j(\mathbf{q})-\Omega). \tag{4}$$

For Eq. (4), the wave vector sum is done with a Brillouin zone sampling method, the z index on $\mathbf{e}^j$ denotes that only the z components of the eigenvectors are included, and the frequencies ω_j are assigned to bins in a histogram. The density of states is closely related to the response determined in the inelastic neutron scattering experiment[9] and also provides a summary of the information contained in the $3N^2$ dispersion curves for the unit cell with N^2 atoms.

For the Ar/graphite model, there are 25 atoms in the Bravais cell and the maximum difference in heights z for the configuration of the minimum potential energy is ≈ 0.085 Å. The S-mode spectral strength for ^{36}Ar is centered at 6.0 meV and has a full width at half maximum (FWHM) of 0.2 meV. This reproduces the result of the analysis[9] of the inelastic neutron scattering from a polycrystalline sample.

For the Kr/graphite model,[27] there are 100 atoms in the Bravais cell and the maximum difference in heights z for the configuration of minimum potential energy is ≈ 0.085 Å. The S-mode spectral strength is centered at 4.25 meV and has a FWHM of 0.2 meV. This agrees with the inelastic atom scattering data.[10]

Both these results are consistent with calculations of the curvature $\partial^2 V_h/\partial z^2$ of the holding potential at the heights of minima at high-symmetry points of the graphite unit cell. The curvature at the center $\vec{r}=0$ is within 2% of the value at a top site $\vec{r}=(\vec{a}_1+\vec{a}_2)/3$. When the calculations for V_h are examined in more detail, it is found that there is a 35% change in the curvature of V_0 (''anharmonicity'') which is almost completely offset by the change in the contributions from the V_g. This is not an automatic result for such potentials, because the corresponding changes reinforce for a widely used model[28] of Xe/Pt(111).

A related system is Xe/graphite. The S mode for the $\sqrt{3}$-commensurate lattice has been observed[29] by inelastic helium atom scattering. As expected, there is no dispersion in $\omega_\perp$ apart from effects of hybridization with the substrate modes near the Brillouin zone center. The incommensurate monolayer has been imaged by scanning tunneling microscopy,[4] which gives an estimate $\Delta z \approx 0.15$ Å for the variation in Xe heights. This value is voltage and tip dependent, but it is on the scale of an estimate of 0.05–0.08 Å from models similar to those used here for argon and krypton.

III. MONOLAYER H_2 ON MgO(001)

A. Geometry

Two HOC lattices of monolayer $H_2/MgO(001)$ are treated in this paper, the $c(4\times2)$ and $c(6\times2)$ with three and five molecules per unit cell, respectively. In this subsection the geometry of the space and reciprocal lattices is specified.[12] The space lattice for the $c(4\times2)$ case is illustrated in Fig. 1.

Denote the unit vectors along the [100] and [010] axes of the MgO surface by $\hat{x}$ and $\hat{y}$ and those along [110] and $[1\bar{1}0]$ by $\hat{\zeta}$ and $\hat{\eta}$. The primitive vectors of the MgO(001) surface are $\ell\hat{\zeta}$ and $\ell\hat{\eta}$, $\ell=2.97$ Å. The primitive vectors of the average H_2 space lattices with long space axes along [110] are

$$\vec{a}_{1,2}=a[\pm\sin(\psi/2)\hat{\zeta}+\cos(\psi/2)\hat{\eta}], \tag{5}$$

with $a\cos(\psi/2)=\ell$ and $a\sin(\psi/2)=\frac{2}{3}\ell$ and $\frac{3}{5}\ell$ for the $c(4\times2)$ and $c(6\times2)$ cases, respectively. That is, on average, they are uniaxially incommensurate lattices with reciprocal lattices spanned by the vectors

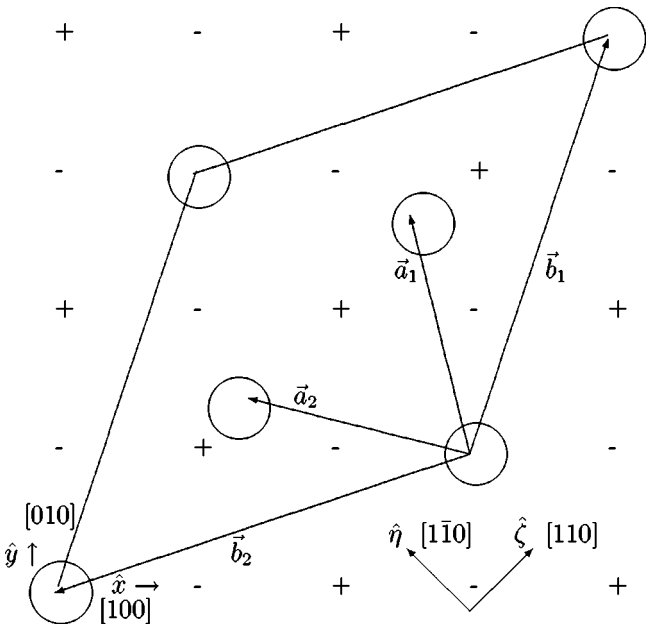

FIG. 1. Schematic of the spatial coordinates for the HOC $c(4\times2)$ lattice of $H_2/MgO(001)$. The primitive vectors $\vec{a}_1$ and $\vec{a}_2$ of the average space lattice and $\vec{b}_1$ and $\vec{b}_2$ of the HOC are shown. The [100], [010], [110], and $[1\bar{1}0]$ azimuths of the MgO substrate are identified. The two sets of Cartesian axes ($\hat{x}$, $\hat{y}$) and ($\hat{\zeta}$, $\hat{\eta}$) are shown. Positive and negative substrate surface ions are denoted + and −, respectively, and the adlayer molecules are denoted ○. The parallelogram gives an outline of the unit cell of the HOC lattice. Corners of the unit cell are situated at + ions, a positioning that is plausible but not yet proved.

$$\vec{\tau}_{1,2}=\tau_0[\pm\cos(\psi/2)\hat{\zeta}+\sin(\psi/2)\hat{\eta}], \tag{6}$$

with $\tau_0=2\pi/a\sin(\psi)$. The primitive space and reciprocal lattice vectors for the HOC $c(4\times2)$ unit cell are

$$\vec{b}_{1,2}=\ell[\pm2\hat{\zeta}+\hat{\eta}], \tag{7}$$

$$\vec{g}_{1,2}=\frac{\pi}{2\ell}[\pm\hat{\zeta}+2\hat{\eta}]. \tag{8}$$

There may be a second domain with a long space axis along $[1\bar{1}0]$; in that case the axes $\hat{\zeta}$ and $\hat{\eta}$ are interchanged in these equations.

The leading reciprocal lattice vectors for the average $c(4\times2)$ lattice have magnitudes 1.906 Å^{-1} and 2.116 Å^{-1}. Both are observed in the $D_2/MgO(001)$ neutron diffraction experiments,[30] the second coincides with an MgO diffraction peak for helium diffraction along the [110] azimuth. The experimental evidence cited[11] for the higher-order cell in the helium diffraction experiment is the peak at $\pi/\ell=1.06$ Å^{-1} along the [110] (or $[1\bar{1}0]$) azimuth and broad peaks along [100] assigned[11] as wings of diffraction peaks along [510] and [310]. Since the [510] peak with projection at 1.87 Å^{-1} $\hat{x}$ arises also for the average lattice, it is the [310] peak with projection at 1.12 Å^{-1} $\hat{x}$ that is distinctive of the HOC cell.

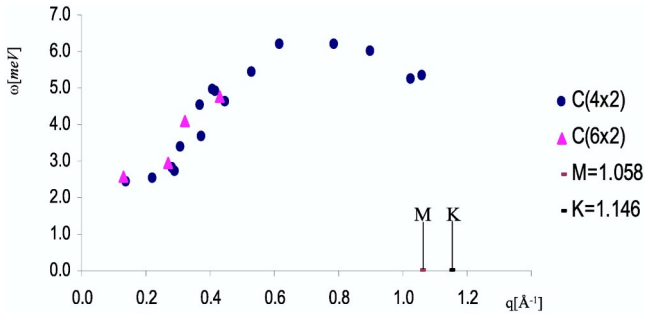

FIG. 2. Dispersive branch of H_2/MgO(001) monolayer solids. The energy $\omega_1(q)$ (in meV) is plotted as a function of wave number q (in Å^{-1}) for the dispersive branch observed (Ref. 11) with inelastic helium atom scattering experiments. The solid circles and triangles denote data for the $c(4\times2)$ and $c(6\times2)$ lattices, respectively. The q values corresponding to the M and K points of the average reciprocal lattice for the $c(4\times2)$ cell are noted on the abscissa. The fact that the data for the two HOC lattices are so similar is support for assigning this phonon branch to in-plane motions polarized primarily along the short axis of the HOC cells. The estimated crossing of this branch and the Rayleigh mode (Ref. 5) of the MgO substrate is at $q\approx0.07$ Å^{-1} and the associated perturbation (Ref. 24) of the adlayer branch is not evident here.

The leading reciprocal lattice vectors for the average $c(6\times2)$ lattice have magnitude 2.056 Å^{-1} and 2.116 Å^{-1}. Both are observed in the D_2/MgO(001) neutron diffraction experiments.[30]

For both the $c(4\times2)$ and $c(6\times2)$ average lattices, a reciprocal lattice vector at $(2\pi/\ell)\hat{\eta}$ coincides with a reciprocal lattice vector of the MgO(001) surface. That term in the adatom-substrate corrugation series adds coherently in the adlayer and causes a zone-center frequency gap for displacements along $\hat{\eta}$. The effect along $\hat{\zeta}$ is expected to be much smaller.

B. Assignment of the dispersive phonon branch

The results of the inelastic helium atom scattering measurements for the [110] azimuth were presented[11] as three phonon branches $\omega_\alpha(q)$, one with a zone-center gap and significant dispersion and two with little dispersion and rather higher energies. While this is suggestive of the three branches expected for a Bravais lattice with one atom/molecule per cell, the analysis here leads to a firm assignment of only one of the observed branches to motion polarized in the ζ-η plane parallel to the surface.

For the $c(4\times2)$ case, the dispersive branch $\omega_1(q)$ measured along [110] has a gap of 2.5 meV at small wave number q, then increases to 6.2 meV at $q=0.6-0.8$ Å^{-1}, and decreases to 5 meV at 1.1 Å^{-1}. The observed dispersive branch for the $c(6\times2)$ case is less complete, partially because of the larger inelastic backgrounds in that case, but Fig. 2 shows that the data for $q=0.15$–0.4 Å^{-1} nearly superimpose on the dispersion curve measured for the $c(4\times2)$. This suggests that the gap in both cases arises from the coherent effect of $g=2\pi/\ell$ in the uniaxially incommensurate average lattices and that the atomic displacements are in-plane motions along the short axis of the HOC cell. The very similar small-q excitations might be transverse oscillations of a domain oriented along [110] or longitudinal oscillations for the alternate domain oriented along $[1\bar{1}0]$ and observed along [110].

The magnitudes of the frequencies $\omega_1(q)$ at small q are consistent with estimates for a monolayer hydrogen solid. Convert the 2.5 meV frequency of the zone-center gap to an estimate of the corrugation amplitude $\bar{V}_g$ for $g=2.12$ Å^{-1} using[2]

$$m\omega_{0\|}^2=-2g^2\bar{V}_g\langle\exp(\imath g\,\eta)\rangle\approx-2g^2\bar{V}_g\exp(-g^2\langle\eta^2\rangle/2). \tag{9}$$

The uncertainty of about 10% in the measured frequencies at small q leads to an uncertainty of 20% in the inferred value of $\bar{V}_g$. With $\langle\eta^2\rangle\approx0.15$ Å^2 from the three-dimensional (3D) solid[31] or monolayer H_2/graphite,[32]the result is $\bar{V}_g\approx-0.47$ meV, as listed in Table I. It is on the scale of the 1.0 meV estimate by Karimi and Vidali,[22] and the experience of Frigo *et al.*[33] was that a similar approximation for other ionic crystals overestimated the corrugation. The strongest argument for assigning the gap to arise from vibrations primarily along the short axis of the HOC cell is the similarity of the branches at small q for both the $c(4\times2)$ and $c(6\times2)$ lattices. Further, if this branch for $c(4\times2)$ were assigned to motions along the long (ζ) axis, there would be two serious problems: (i) To get an appreciable restoring force for the $q=0$ motion along $\hat{\zeta}$ would require large relative displacements of molecules in the HOC unit cell and there is no support for this in eikonal fits to the diffracted intensities.[34] (ii) Fitting the nearly dispersionless branch observed at 8.5 meV to $\hat{\eta}$ motions would give $\bar{V}_g\approx-5.4$ meV, which is very large compared to the H_2/graphite corrugation. It also is large enough that barriers 4 $\bar{V}_g$ to lateral motion of the H_2 on the MgO surface would severely reduce the lateral mobility at temperatures $T\leqslant10$ K. There was no indication of this in the experiments.

Over the rest of the Brillouin zone, $\omega_1(q)$ should have large or even dominant contributions from H_2-H_2 interactions. To make this quantitative, construct a simple model for the in-plane harmonic dynamics of the average $c(4\times2)$ lattice using radial force constants β_1 for the four nearest neighbors at 3.57 Å and β_2 for the two next-nearest neighbors at 3.96 Å. With a parametrization $\beta_j=m\Omega_j^2$, the frequencies for normal modes with longitudinal L and transverse T polarizations relative to $q\hat{\zeta}$ are

$$\omega_{L\zeta}^2(q)=\frac{16}{13}\Omega_1^2[1-\cos(2q\ell/3)]+2\Omega_2^2[1-\cos(4q\ell/3)], \tag{10}$$

$$\omega_{T\zeta}^2(q)=\omega_{0\|}^2+\frac{36}{13}\Omega_1^2[1-\cos(2q\ell/3)], \tag{11}$$

and for those polarizations relative to $q\hat{\eta}$ are

$$\omega_{T\eta}^2(q) = \frac{16}{13}\Omega_1^2[1-\cos(q\ell)], \tag{12}$$

$$\omega_{L\eta}^2(q) = \omega_{0\parallel}^2 + \frac{36}{13}\Omega_1^2[1-\cos(q\ell)]. \tag{13}$$

The coefficients 16/13 and 36/13 arise from the force tensor constructed with Eq. (5). Fitting Eqs. (11) and (13) to $\omega_1 = 6.0$ meV at $q = 0.8$ Å^{-1} gives $\Omega_1 = 3.3$ meV and 2.5 meV, respectively. With such values, the frequencies $\omega_{L\zeta}$ and $\omega_{T\eta}$ would be much smaller than those in the gap branches and in a range where no excitations were observed in the experiments.[11] It would be ambiguous from the experimental data whether the gap branches for one or both of the $c(4\times2)$ domains had been observed.

However, $\Omega_1 \approx 3$ meV is quite small in the light of values[31] for the 3D isotopic hydrogen solids. The zone-boundary phonons from inelastic neutron scattering experiments[31] on ortho-D_2 at $L_{nn} = 3.61$ Å and 3.53 Å can be fit to a radial force constant that gives $\Omega_1 \simeq 5.0$ meV for H_2 at these separations. A fit to the data[31] for para-H_2 at $L = 3.79$ gives $\Omega \simeq 3.5$ meV. The 3.96 Å neighbors in the $c(4\times2)$ lattice are at even larger separation and the Ω_2 value would be even smaller; therefore that term is dropped from Eq. (10) in the following discussion.

When the parameter set of $\omega_{0\parallel} = 2.5$ meV, $\Omega_1 = 5.0$ meV, and $\Omega_2 = 0$ is used in Eqs. (10)–(13), the identification of $\omega_1(q)$ with the gap mode $\omega_{T\zeta}$ or $\omega_{L\eta}$ remains valid only at small q. For $q = 0.7$–1.1 Å^{-1} those branches have frequencies in the range 8–12 meV and the gapless modes have frequencies in the range 5–8 meV. What has been viewed as a single branch $\omega_1(q)$ would have to be treated as a coincidental combination of gap and gapless modes. The situation remains very similar when $\Omega_1 = 4.0$ meV is used. The in-plane motion with 8–12 meV frequencies would help resolve the difficulty of assigning the two dispersionless branches discussed in the next subsection. This is not a complete resolution because $\omega_{T\zeta}$ and $\omega_{L\eta}$ are both less than 4.0 meV at $q < 0.4$ Å^{-1}, a q range where both higher-frequency branches are observed. Most critically, there are no observed phonons with the frequencies of 6.5–8.0 meV that are part of the calculated range for $\omega_{T\zeta}$ and $\omega_{L\eta}$. The radial force constants for $\Omega = 5.0$ and 3.0 meV differ by more than a factor of 2. It would be a surprise if the fitting to the 3D solids gave an effective monolayer force constant that much in error, but this is a step that could be tested with quantum solid calculations.

The present situation is either that the radial force constant in the $c(4\times2)$ monolayer is much smaller than expected or that, for some unknown reason, substantial ranges of the monolayer phonon spectra were not accessed in the experiment.[11,35]

C. Dispersionless branches

Two nearly dispersionless branches are observed[11] for both the HOC monolayer lattices. For $c(4\times2)$, the branches are at approximately 8.5 and 10.5 meV. For $c(6\times2)$, they are at approximately 9.0 and 11.0 meV.

Karimi and Vidali predict[22] an excitation energy of ≈ 10.5 meV for H_2/MgO in the laterally averaged potential V_0, as in selective adsorption resonances. Scaling the known excitation[36] for H_2/graphite by the square root of the ratio of adsorption energies[14] on graphite and MgO gives an estimate 12–12.5 meV. Thus, one of the observed branches probably is the S mode $\omega_\perp(q)$ of H_2/MgO. The puzzle is the appearance of two modes in this energy range.

One possibility that arises for the $c(4\times2)$ HOC cell is that there might be two heights for molecules in the cell, one for those (a) at $0\hat{\zeta}$ and another for those (b) at $(4/3)\ell\hat{\zeta}$ and $(8/3)\ell\hat{\zeta}$ where the leading corrugation energies are equal. An eikonal analysis[11,34] of the helium scattering data admits height differences $\Delta z = \overline{z_b} - \overline{z_a}$ of 0.15–0.23 Å. However two calculations based on this mechanism, to be described in the next paragraphs, do not succeed in generating a 20% splitting in $\omega_\perp$.

First, there is a classical force relaxation to find minima of z potentials at a and b,

$$V_a(z) = V_0(z) + 4\overline{V}_g \exp(-gz), \tag{14}$$

$$V_b(z) = V_0(z) + \overline{V}_g \exp(-gz), \tag{15}$$

where a common approximation for the z dependence of the corrugation is used.[37] Anharmonicity is included in V_0 through the approximation

$$V_0(z) = \frac{1}{2}Kz^2[1-\alpha z], \tag{16}$$

based on a Morse potential. Fits to the energy levels observed[36] for H_2/graphite and calculated[22] for H_2/Mgo(001) give $\alpha = 1.2$–1.3 Å^{-1}. Then the curvatures at the two minima give perpendicular frequencies that differ by less than 5% for Δz in the range 0.1–0.22 Å. A calculation that omits the anharmonicity in V_0 does give two frequencies differing by about 20% and with $\omega_{0\parallel} = 4$–4.5 meV. As argued in Sec. II, it is inconsistent and leads to nonphysical effects in the classical monolayer solids, to include only the change in curvature arising from the corrugation terms.

The second calculation is to solve for the ground-state and first excited-state energies of the potentials V_a and V_b using for V_0 a Morse potential fit to the three levels calculated by Karimi and Vidali.[22] The scale for $\overline{V}_g$ is set by fitting to values $\omega_{0\parallel} = 2.5$–$4.0$ meV. That such a calculation is required is suggested by the fact that the Δz inferred from the eikonal analysis is less than the root-mean-square spread in heights[32] for H_2/graphite. However, even in the most corrugated case, the calculated difference in heights is only 0.07 Å and the difference in excitation energies only 7%.

Both these calculations are limited by the *ad hoc* character of the model potentials, but they show the difficulty in reproducing the observed dispersionless branches. With more realistic models for the holding potential $V_h(\vec{r},z)$ other possibilities might be explored, such as the differences for $p-H_2$ and $o-H_2$ which are known[32] to be appreciable for the vibrational spectrum of the monolayers on graphite.

Finally, there is one further dispersionless branch observed for the H_2 layers on MgO(001). A branch with 5.5 ± 0.5 meV is attributed[11,34] to perpendicular vibrations of molecules in the second layer of a bilayer film. This presents a rather different but quite compelling problem: for the classical inert gases Ar, Kr, and Xe on Ag(111) and Pt(111), the $\omega_\perp$ of the bilayer typically[7,8] has a dispersion of 30%–40% over the Brillouin zone. Calculations[38] for H_2 films show that the top layer is quite easily disordered, but there has been no demonstration that this would lead to the type of frequency spectrum that is reported for bilayer H_2/MgO.

IV. CONCLUSIONS

The ''2D approximation'' in which monolayer solids are assumed to be planar has been justified mostly by after-the-fact comparisons with experimental data. The conclusion here is that the successes were based partially on offsetting anharmonicities in components of the adatom-substrate potential. The monolayer does have a z topography that can be evidenced by imaging or reflected in diffracted intensities. However, when the effect of the z variations is combined with the offsetting anharmonicities, the $\omega_\perp(q)$ branch remains nearly dispersionless. This was verified with calculations for classical monolayers and is consistent with an *ad hoc* model for a quantum monolayer.

One of the observed phonon modes of the quantum monolayer solid $H_2/MgO(001)$ can definitely be assigned, for small q, as the spectrum of motion along the simply commensurate axis of the lattice and the fitted corrugation amplitude is plausible in the light of data for H_2/graphite. The two nondispersive branches present a puzzle because, although an $\omega_\perp$ branch was predicted for that energy range, no satisfactory mechanism for the splitting into two branches has been given yet. The nondispersive branch assigned in the experiments to a H_2 bilayer also stands as a puzzle because the classical bilayer systems show substantial dispersion. Much of the discussion for the H_2 solid given here has a preliminary character because full quantum solid calculations combining lateral and perpendicular motions[32,39] have not been performed for $H_2/MgO(001)$. It is hoped that this paper helps to focus the problems posed by the $H_2/MgO(001)$ system for future efforts.

ACKNOWLEDGMENTS

It is a pleasure to thank Dr. F. Traeger for many helpful discussions. I also thank her and Professor H. Taub for their comments on the manuscript. This work has been partially supported by Grant No. NSF-DMR0104300.

[1] L. W. Bruch, A. P. Graham, and J. P. Toennies, J. Chem. Phys. **112**, 3314 (2000), and references contained therein.
[2] L. W. Bruch, Phys. Rev. B **49**, 7654 (1994).
[3] F. Brunet, R. Schaub, S. Féderigo, R. Monot, J. Buttet, and W. Harbich, Surf. Sci. **512**, 201 (2002).
[4] B. Grimm, H. Hövel, M. Pollmann, and B. Reihl, Phys. Rev. Lett. **83**, 991 (1999); H. Hövel (private communication).
[5] G. Benedek, G. Brusdeylins, V. Senz, J. G. Skofronick, J. P. Toennies, F. Traeger, and R. Vollmer, Phys. Rev. B **64**, 125421 (2001); F. Traeger (private communication) applied this analysis also to He-$H_2/MgO(001)$. This included the Beeby correction for an attractive well of depth 3 meV and an angle-factor following U. Garribaldi, A. C. Levi, R. Spadacini, and G. Tommei, Surf. Sci. **48**, 649 (1975), Eq. (B.20). Note that the diffracted intensities depend more on the repulsive portion of V_h than on its attractive well. For some cautionary remarks on use of the eikonal analysis to estimate the topography of strongly corrugated systems, see A. Šiber and B. Gumhalter, *ibid.* **529**, L269 (2003).
[6] L. W. Bruch and A. D. Novaco, Phys. Rev. B **61**, 5786 (2000).
[7] K. D. Gibson and S. J. Sibener, Phys. Rev. Lett. **55**, 514 (1985); Faraday Discuss. Chem. Soc. **80**, 203 (1985); J. Chem. Phys. **88**, 7893 (1988).
[8] P. Zeppenfeld, U. Becher, K. Kern, and G. Comsa, J. Electron Spectrosc. Relat. Phenom. **54**, 265 (1990).
[9] H. Taub, K. Carneiro, J. K. Kjems, L. Passell, and J. P. McTague, Phys. Rev. B **16**, 4551 (1977).
[10] J. Cui, D. R. Jung, and R. D. Diehl, Phys. Rev. B **45**, 9375 (1992).
[11] J. G. Skofronick, J. P. Toennies, F. Traeger, and H. Weiss, Phys. Rev. B **67**, 035413 (2003).
[12] L. W. Bruch, M. W. Cole, and E. Zaremba, *Physical Adsorption: Forces and Phenomena* (Oxford University Press, Oxford, 1997).
[13] The potential models used by G. Vidali, M. W. Cole, and J. R. Klein, Phys. Rev. B **28**, 3064 (1983), have distinctly smaller σ values for the Ar-graphite and Kr-graphite cases. Then the calculated corrugations for the isotropic interactions are larger, and the empirical need for including the γ_R term is less evident [G. Vidali and M. W. Cole, *ibid.* **29**, 6736 (1984)]. The isotropic models used in the present work are chosen because they have been used in modeling of the monolayer solids and because it seems more consistent to include estimates of the effect of the substrate anisotropy on both the attractive and repulsive terms of the potential. This procedure has been discussed previously for the series He, Ne, and Kr on graphite: L. W. Bruch, in *Phase Transitions in Surface Films II*, edited by H. Taub, G. Torzo, H. J. Lauter, and S. C. Fain, Jr. (Plenum, New York, 1991), p. 67.
[14] G. Vidali, G. Ihm, H.-Y. Kim, and M. W. Cole, Surf. Sci. Rep. **12**, 133 (1991).
[15] L. W. Bruch, A. P. Graham, and J. P. Toennies, Mol. Phys. **95**, 579 (1998).
[16] J. Braun, D. Fuhrmann, A. Šiber, B. Gumhalter, and Ch. Wöll, Phys. Rev. Lett. **80**, 125 (1998).
[17] Ch. Ramseyer, V. Pouthier, C. Girardet, P. Zeppenfeld, M. Büchel, V. Diercks, and G. Comsa, Phys. Rev. B **55**, 13 203 (1997). See also Ch. Boas, M. Kunat, U. Burghaus, B. Gumhalter, and Ch. Wöll, *ibid.* **68**, 075403 (2003).
[18] F. Y. Hansen, V. L. P. Frank, H. Taub, L. W. Bruch, H. J. Lauter, and J. R. Dennison, Phys. Rev. Lett. **64**, 764 (1990).

[19] H. J. Lauter, H. Godfrin, and P. Leiderer, J. Low Temp. Phys. **87**, 425 (1992).

[20] There is a determination of $V_{g0}=-0.28$ meV for ^{4}He/graphite from band structure effects in selective adsorption resonance data [M. W. Cole, D. R. Frankl, and D. L. Goodstein, Rev. Mod. Phys. **53**, 199 (1981)].

[21] M. Caragiu, Th. Seyller, and R. D. Diehl, Surf. Sci. **539**, 165 (2003); Th. Seyller, M. Caragiu, R. D. Diehl, P. Kaukasoina, and M. Lindroos, Phys. Rev. B **60**, 11 084 (1999), and references contained therein.

[22] M. Karimi and G. Vidali, Phys. Rev. B **39**, 3854 (1989); G. Vidali and M. Karimi, Langmuir **5**, 612 (1989).

[23] C. G. Shaw, Ph.D. thesis, University of Washington–Seattle, 1979.

[24] B. Hall, D. L. Mills, P. Zeppenfeld, K. Kern, U. Becher, and G. Comsa, Phys. Rev. B **40**, 6326 (1989).

[25] K. L. D'Amico, J. Bohr, D. E. Moncton, and D. Gibbs, Phys. Rev. B **41**, 4368 (1990).

[26] In this work, the substrate is treated as static. Although there is an adsorbate-substrate potential energy, there is no provision for the hybridization (Refs. 7 and 24) of adlayer and substrate dynamics that occurs close to the adlayer Brillouin zone center for some degrees of freedom.

[27] H. J. Lauter, V. L. P. Frank, H. Taub, and P. Leiderer, Physica B **165-166**, 611 (1990), report a zone-center gap of 0.75 meV for $\sqrt{3}$-Kr/graphite. That gap leads to an estimate of $V_{g0}\approx-0.44$ meV which is barely enough to stabilize the commensurate lattice and is much smaller than the value $V_{g0}\approx-1.0$ meV for the model used in Sec. II.

[28] J. A. Barker and C. T. Rettner, J. Chem. Phys. **97**, 5844 (1992); **101**, 9202(E) (1994).

[29] J. P. Toennies and R. Vollmer, Phys. Rev. B **40**, 3495 (1989).

[30] D. Degenhardt, H. J. Lauter, and R. Haensel, Jpn. J. Appl. Phys., Suppl. **26**(3), 341 (1987).

[31] M. Nielsen, Phys. Rev. B **7**, 1626 (1973).

[32] W. B. J. M. Janssen, T. M. H. van den Berg, and A. van der Avoird, Phys. Rev. B **43**, 5329 (1991); Surf. Sci. **259**, 389 (1991).

[33] A. Frigo, F. Toigo, M. W. Cole, and F. O. Goodman, Phys. Rev. B **33**, 4184 (1986).

[34] F. Traeger (private communication) noted that a small lateral displacement (<0.1 Å) had an effect similar to that of a 10%–20% change in the corrugation. She added a sinusoidal corrugation for the H_2-MgO(001) topography to a model for the He-H_2 corrugation and found the H_2-MgO(001) amplitude to be 0.22–0.28 Å by fitting He-H_2/MgO(001) diffraction intensities. She had found an amplitude 0.26–0.3 Å in an analysis of H_2-MgO(001) scattering of ortho-H_2 molecules in the $j=1$, $m=\pm1$ state.

[35] A more extreme resolution would be that the $c(4\times2)$ structure identified (Ref. 30) in neutron diffraction for D_2/MgO(001) has not been replicated for H_2/MgO(001) and that the dispersion curves from the inelastic helium scattering are for a more dilated, but still uniaxially incommensurate, monolayer solid. The observation of signatures for the $c(4\times2)$ to $c(6\times2)$ transition for D_2, HD, and H_2 in adsorption isotherms at about 18 K gives some evidence against this proposal. See O. E. Vilches, F. C. Liu, D. L. Kingsbury, J. Ma, M. Bienfait, J. Suzanne, J. M. Gay, M. Maruyama, P. Zeppenfeld, D. Degenhardt, H. J. Lauter, F. Rieutord, and G. Coddens, in *Excitations in Two-Dimensional and Three-Dimensional Quantum Fluids*, edited by A. F. G. Wyatt and H. J. Lauter (Plenum, New York, 1991), p. 477.

[36] L. Mattera, F. Rosatelli, C. Salvo, F. Tommasini, U. Valbusa, and G. Vidali, Surf. Sci. **93**, 515 (1980).

[37] For matching to Eq. (9), the $\overline{V_g}$ in Eqs. (14) and (15) is an effective amplitude that includes the factor $\exp(-g^2\langle\eta^2\rangle/2)$ and the force constant for $\omega_{0\|}$ is a weighted average of the contributions from the *a* and *b* sites of the HOC unit cell. The assumed exponential dependence is consistent with the large difference for the corrugation amplitudes of Xe/Cu at two values of *g* in Table I.

[38] M. Wagner and D. M. Ceperley, J. Low Temp. Phys. **94**, 161 (1994).

[39] K. Nho and E. Manousakis, Phys. Rev. B **65**, 115409 (2002).